Meccanica **30:** 577–589, 1995.

Finite-Scale Microstructures and Metastability in One-Dimensional Elasticity

LEV TRUSKINOVSKY[1] and GIOVANNI ZANZOTTO[2]
[1]*University of Minnesota, Department of Aerospace Engineering and Mechanics; Minneapolis, MN, U.S.A.*
[2]*Università di Padova, Dipartimento di Metodi e Modelli Matematici per le Scienze Applicate; Padova, Italy*

(Received: 31 October 1994; Accepted: 31 December 1994)

Abstract. This paper addresses the non-uniqueness pointed out by Ericksen in his classical analysis of the equilibrium of a one-dimensional elastic bar with non-convex energy [1]. Following some previous work in this area, we suitably regularize the problem in order to investigate this degenerancy. Our approach gives an explicit framework for the the study of the rich variety of *finite-scale* equilibrium microstructures for the bar in a hard loading device, and their stability properties. In this way we clarify the role of interfacial energy in creating finite-scale microstructures, by considering the combined effect of the oscillation-inducing and oscillation-inhibiting terms in the energy functional.

Sommario. Il lavoro riguarda la non unicità messa in luce da J.L. Ericksen nella sua analisi dell'equilibrio di barre elastiche con energia non convessa. Seguendo le linee di precedenti lavori, per investigare questa degenerazione si ricorre ad una regolarizzazione del problema e si dà un esplicito quadro di riferimento per lo studio della ricca varietà delle microstrutture di scala finita e della loro stabilità. Si chiarisce in particolare il ruolo dell'energia di interfaccia nella creazione di microstrutture di scala finita considerando l'effetto combinato di termini inibitori e favorevoli all'insorgere di oscillazioni nel funzionale energia.

Key words: Microstructures, Interface energy, Non convex variational problems, Phase transitions, Solid mechanics.

1. Introduction

Experimental observations of stress- and deformation-induced phase transitions and twinning in solids reveal fine layered microstructures in a great variety of configurations. Typical examples of observed phase arrangements include rather regular patterns due to piecewise homogeneous layering of twins in fine bands (see Figure 1). Ericksen's analysis [1] of the highly non-unique absolute minimizers for a one-dimensional elastic bar with a non-monotone stress-strain relation showed how nonlinear elasticity could be used for the modeling of phenomena of this kind. Later development of these ideas, especially in a three-dimensional context, greatly improved the understanding of the mechanisms leading to the formation of fine microstructures in solid-to-solid transformations (see [2] for a recent review). However, the absolute minimization of the elastic energy cannot predict some important features of the transitions, and for this reason it is interesting to investigate also the *local* minimizers of the energy.

In this paper we briefly report about the result of a forthcoming work [3], in which we give a framework for the detailed investigations of the variety of stable and metastable equilibria of a simple system, for a wide range of imposed boundary conditions. We consider a one-dimensional bar containing a 'mixture' of two homogeneous elastic components. One component may describe the austenitic phase of a multiphase elastic material, while the other corresponds to a homogenized fine layering of different variants of the martensitic

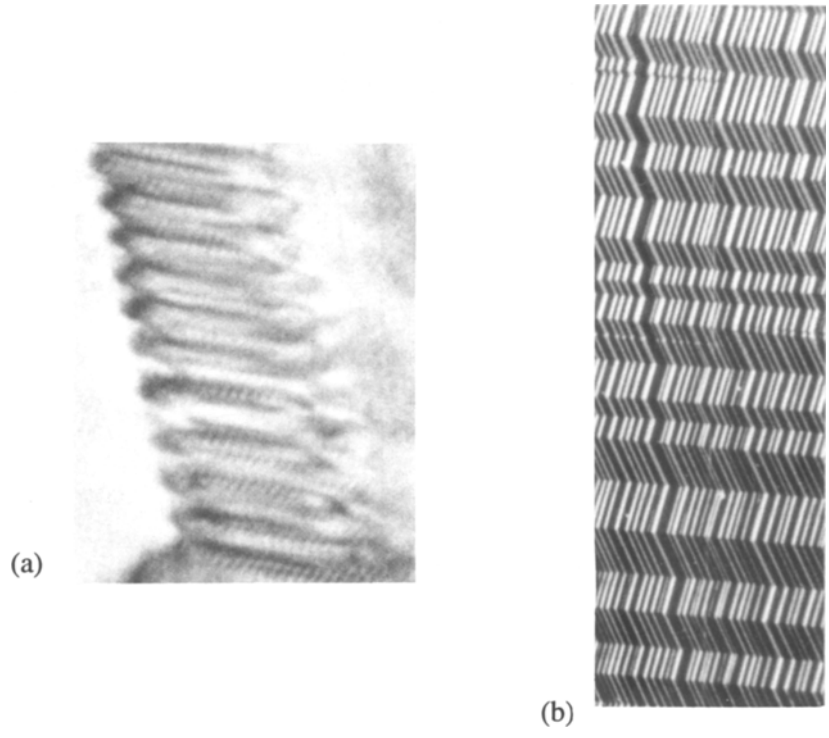

Fig. 1. (a) Multiply winned nanometer size plate of Ni_5Al_3 growing in B2 austenite (from Schryvers *et al.* [12]. (b) Internal martensitic twins in a $CuAl_{14}Ni_{4,2}$ (wt %) shape-memory single crystal (from Tan and Xu [13]).

phase of the same substance. The bar interacts with an elastic substratum which mimicks the three-dimensional boundary conditions constraining surface displacements. This includes microstructural refinement, whereas the 'surface tension' contribution to the energy drives the system to minimizing the number of phase interfaces (a similar model has already been considered in the literature, (see [4], [5]). We develop our main considerations under fairly general constitutive assumptions, and we find that the elastic and phase-equilibria for the bar in a hard loading device can be obtained by piecing together smooth solutions of ODEs, according to appropriate jump and boundary conditions. This allows for the study of the energy landscape in the infinite dimensional space, which can be made explicit at least in the case of a quadratic energy density for each phase.

The expectation that our elementary model will in fact give interesting insight about finite-scale microstructures is supported by the analysis of S. Müller [4], [5]. For a special case of boundary conditions and under the assumption of a smooth two-well energy, he determined the asymptotic behaviour for the number of interfaces in the absolute minimizer, in the limit of vanishing surface tension and finite stiffness of the substratum. What is most remarkable, he could also prove the periodicity of the minimizers, which of course is not the case for the general boundary conditions we consider.

Our analysis complements S. Müller's in that we focus on the local minimizers of the energy and extend the range of boundary conditions. This allows us to address a number of interesting questions that are still quite unclear regarding the general theory of phase transitions in solids, and about which the existence of finite-scale metastable microstructures is likely to have great relevance. One issue is for instance the markedly hysteretic behaviour which is typical for

solids undergoing phase transformation. As is well-known, the study of absolute minimizers cannot account for the hysteresis in the load-deformation curves observed experimentally [6], [7], [8], while the material getting locked in metastable states is a likely cause of such phenomena. A clear suggestion about this comes for instance from the calculations regarding a discrete system of bistable elements (snap-springs) by Fedelich and Zanzotto [9]. Other questions that our model allows us to address include the formation of *finite nuclei* as a mechanism for microstructure refinement, and the assessment of the enrgy barriers between different equilibrium configurations.

2. The Model

2.1. Energy

Denote by $u(x)$ the displacement of the reference point x of a bar $[0, 1]$ containing a 'mixture' of two homogeneous elastic components, say '+' and '−' (the two 'phases' of the material); their energy densities are given by smooth convex functions of the strain u':

$$f = f_+(u') \quad \text{and} \quad f = f_-(u'). \tag{2.1}$$

We suppose that the total energy functional is given by the sum of three terms:

$$E = \int_0^1 [\chi f_-(u') + (1-\chi) f_+(u')]\mathrm{d}x + \alpha \int_0^1 (u'')^2 \mathrm{d}x + \beta \int_0^1 u^2 \mathrm{d}x, \tag{2.2}$$

where χ denotes the volume fraction of the '−' phase. the first term in (2.2) gives the amount of elastic energy stored in the bar as the integral of the energy density per unit reference length. We assume that the two components are seperated; therefore, in (2.2) we assume that χ is the characteristic function of the subset of $[0, 1]$ occupied by the '−' component. The second term in (2.2) is a gradient-dependent 'interfacial' energy, in which $\alpha > 0$ is a constant providing an internal length-scale proportional to $\alpha^{1/2}$. Finally, the third term in (2.2) describes the energy stored in an elastic substratum due to the deformation of the bar, which introduces a further length-scale, proportional to $\beta^{-1/2}$.

2.2. The Functional

We carry out our study under some simplifying assumptions. First, in order to concentrate our attention only on the physically most relevant solutions, we only allow for arrangements in which the region occupied by each phase is a *finite* union of intervals. Thus we consider a finite number N of points c_i in $[0, 1]$, $i = 1, \ldots, N$, such that $c_i < c_{i+1} (c_0 \equiv 0,\ c_{N+1} \equiv 1)$, and require χ in (2.2) to be the characteristic function of the subsets $[0, c_1] \cup [c_2, c_3] \cup \cdots$ or $[c_1, c_2] \cup [c_3, c_4] \cup \cdots$ of $[0, 1]$. Each point c_i gives the position of a *phase-boundary* in the bar, where a switching of components, that is, of energy functions (see (2.1)), occurs.

Confining our attention to extremals and competitors with a finite number of transition points replaces the unknown function χ in (2.2) by finite sets of variables $c_1, \ldots, c_N$; their number N then acts as a discrete parameter. The energy functional becomes explicitly

$$E = \begin{cases} E_0[u], \\ E_1[u,\, c_1], \\ \quad \cdot \\ \quad \cdot \\ \quad \cdot \\ E_N[u,\, c_1, \ldots, c_N], \\ \quad \cdot \\ \quad \cdot \\ \quad \cdot \\ \qquad (N = 0, 1, 2, \ldots) \end{cases} \tag{2.3}$$

whose infinitely many 'branches' are each given by

$$E_N[u,\, c_1, \ldots, c_N] = \sum_{h=0}^{N} \int_{c_i}^{c_{i+1}} [f_{\pm}(u') + \alpha(u'')^2 + \beta u^2] \mathrm{d}x. \tag{2.4}$$

In the integral (2.4) it is understood that the functions f_- and f_+ are taken alternately in each interval $[c_i, c_{i+1}]$.

2.3. Boundary conditions

The (symmetric) boundary conditions to be met by all displacements in the hard device are given by

$$u(0) = -d/2, \quad u(1) = d/2. \tag{2.5}$$

In (2.5) the parameter d has the meaning of a normalized measure of the imposed displacements at the ends of the pinned bar. Since we are indeed considering the normalized interval [0, 1], d can also be interpreted as a measure of the average strain in the bar.

3. Local and Absolute Minimization of the Energy

3.1. Local minimization: elastic and phase-equilibria

The particular structure of our energy functional naturally lends itself to a step-wise minimization which breaks down the process into several stages.

Let d and N be given; we first look for minimizers $[u, c_i]$ of E_N with fixed N. These will in turn be obtained by first calculating the extremals of E_N with fixed N. Such extremals are the *phase-equilibria* of the bar, which belong to separate branches in the space of admissible displacements ('u-space'); each branch is indexed by the number N of phase-boundaries, and is parameterized by d ('N-branches' of equilibria). Extremals in an N-branch only give candidate minimizers, and it is necessary to investigate separately the *stability* of each phase-equilibrium. After this is determined, total minimization of (2.3) is achieved by considering also competitors belonging to different N-branches, i.e. with a different number of transition points.

In order to study the stability of phase-equilibria, we take advantage of two features of our model: the convexity of f_+ and f_- and the description in terms of c_i. This indeed decouples, for each N, a relevant finite-dimensional part of the problem, where all the non-convexity is present, from the remaining infinite-dimensional setting in which the problem is convex. This decoupling has a clear physical meaning (possibility of 'frozen' or 'slow moving' interfaces).

Owing to the convexity of f_+ and f_-, the displacement u can be minimized out of E_N; doing so amounts to introducing, before actually considering phase-equilibria, another important class of configurations: the *elastic equilibria* of the bar. These are extremals of the energy (2,4) with the constraint that the position of the interfaces c_i be fixed in [0,1].

Now, given any c_i, N, and d in their appropriate ranges, it is possible to show that up to symmetries not affecting the energy, a unique elastic equilibrium u_{d,c_i} exists, which the convexity hypotheses guarantee is the absolute minimizer of the energy against competitors with the same N and c_i.

For each N, u is minimized out of E_N so as to obtain $E_N^*(c_i, d)$, which describes the energy landscape of the bar in elastic equilibrium:

$$E_N^*(c_i, d) = E_N[u_{d,c_i}, c_i], \text{ for } N = 0, 1, \ldots. \tag{3.1}$$

The uniqueness of elastic equilibria implies that, for each N, E_N^* is a single-valued function of the imposed deformation and of the position of the interfaces.

The investigation of the stability properties of phase-equilibria belonging to an N-branch can now be done through the study of the minimizers of the functions E_N^*, $N = 0, 1, \ldots$, each of which just depends on a finite number of variables. Finding the extremals of $E_N[u_{c_i}, c_i]$ in the class of all elastic equilibria with variations of the points c_i (for fixed N), we indeed obtain the values of the c_i's giving phase-equilibria as *critical points* of E_N^*, whose stability can be assessed as usual. This allows us to eliminate the variables c_i from (3.1), and to obtain the energy E_N^{**} of extremals as a function of d only. Denote by u_d the phase-equilibria belonging to an N-branch, and by $c_i(d)$ the position of the interfaces in u_d as functions of d; the *phase-equilibrium energy* of the bar in the elastic foundation is:

$$E_N^{**}(d) = E_N^*(c_i(d), d) = E_N[u_d, c_i(d)], \text{ for } N = 0, 1, \ldots. \tag{3.2}$$

Its d-derivative $\Sigma_N^{**}(d)$ gives the phase-equilibrium *stress–strain relation* of our system. For any given N, phase-equilibria at given d are in general, unlike elastic equilibria, not unique (nor are they always minimizers). Each N-branch of phase-equilibria thus splits into 'sub-branches' with same N; this in turn means that each N-branch of the phase-equilibrium energy E_N^{**} and of the stress–strain diagram will be multi-valued.

3.2. Absolute Minimizaton; Phase Diagram

The final minimization of the energy now takes place among all the branches of E_N^{**}. Taking into account also the presence of the physical parameters α and β which affect the features of the functions introduced above, absolute minimization now gives an integer-valued function $N(d, \alpha, \beta)$ - a 'staircase' for each d, or for each α and β. In each appropriate region of the (d, α, β)-space, $N(d, \alpha, \beta)$ indicates which one among the N-branches of solutions is the most stable: this is the *phase-diagram* of the bar. By means of $N(d, \alpha, \beta)$, the *absolute-minimum energy* is obtained, as a single-valued function:

$$E^{***}(d, \alpha, \beta) = E^{**}_{N(d,\alpha,\beta)}(d, \alpha, \beta); \tag{3.3}$$

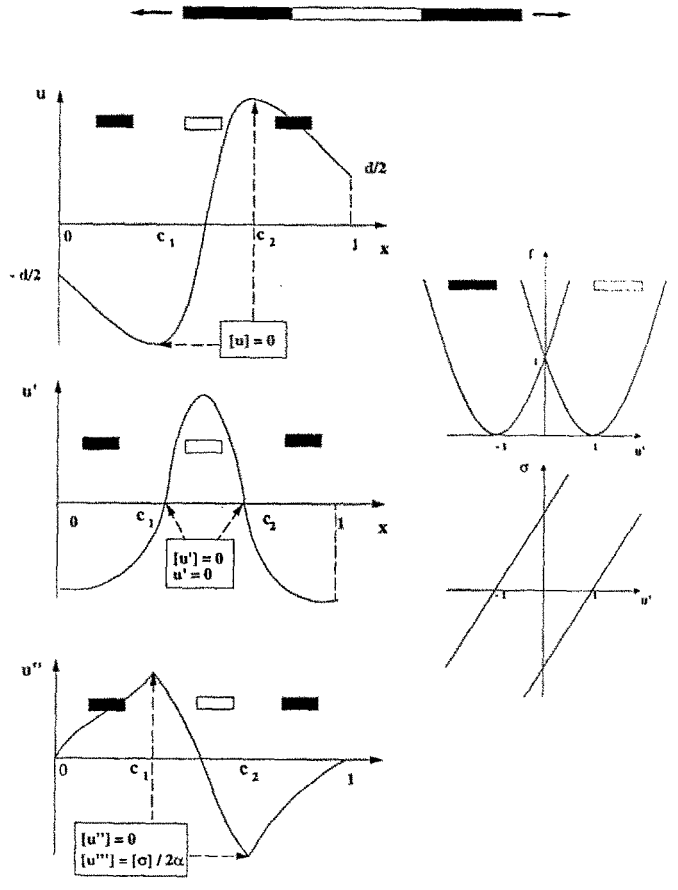

Fig. 2. The generic profile of an extremal with two transition points ($N = 2$), and of its first and second derivatives, in the case of the bilinear material considered in Section 4. The equilibrium positions of the interfaces coincide with the zeros of the strain, where there is reduced smoothness of the solutions (jump in the third derivative).

its d-derivative $\Sigma^{***}(d, \alpha, \beta)$ gives the generalized *Maxwell line* in the stress–strain diagram $\Sigma_N^{**}(d)$. The functions $E_N^{**}(d)$ and $E^{***}(d)$ (and their d-derivatives) will be referred to as the 'macroscopic' or 'effective' energy (and stress–strain relations) of the bar.

3.3. Explicit conditions for extremals

By using some classical arguments of variational calculus, it is possible to see that the extremals are obtained by piecing together smooth solutions of ODEs, according to suitable jump conditions. Explicitly, in our problem the conditions characterizing the phase-equilibria $[u, c_i]$ subject to (2.5) are the following (see Figure 2 for the case of quadratic energies as in Section 4):

(i) The displacement u is of necessity at least of class C^2 in [0,1], and the intervals $[c_i, c_{i+1}]$, $i = 0, \ldots, N$, it satisfies the Euler–Lagrange equation:

$$2\alpha u'''' - f''_{\pm}(u')u'' + 2\beta u = 0 \tag{3.4}$$

where it is understood that f''_+ or f'_- are taken in each interval, as in (2.4).

(ii) At the transition points c_h, $h = 1, \ldots, N$, the following must hold:

$$\begin{aligned} &[\![u'']\!]_{c_h} = 0 \qquad \text{(balance of moments)}, \\ &[\![f'_{\pm}(u') - 2\alpha u''']\!]_{c_h} = 0 \quad \text{(balance of stresses, including couple stresses)}, \end{aligned} \tag{3.5}$$

and

$$[\![f_{\pm}(u')]\!]_{c_h} = 0 \qquad \text{(Maxwell condition)} \tag{3.6}$$

where $[\![A]\!]_x = A(x^+) - A(x^-)$ denotes the discontinuity at x of any quantity A.

(ii) In addition to the imposed boundary conditions (2.7), the extremals must also satisfy:

$$u''(0) = 0, \quad u''(1) = 0. \tag{3.7}$$

We recall the further jump conditions at the transition points that hold because all displacement are C^1:

$$[\![u']\!]_{c_h} = 0, \quad [\![u]\!]_{c_h} = 0 \quad \text{(smoothness conditions)}. \tag{3.8}$$

Conditions (3.4–3.8) and (2.5) characterize phase-equilibria, while elastic equilibria do not necessarily satisfy the 'Maxwell condition' (3.6); this means that there is a jump in energy at the transition points. Equation (3.6) is an explicit form of the critical-point condition for the 'finite-dimensional' elastic energy E_N^* defined in (3.2):

$$\frac{\partial E_N^*}{\partial c_h} = -[\![f_{\pm}]\!]c_h = 0. \tag{3.9}$$

4. The case of Quadratic Energies

4.1. Computation of the extremals

In the case of quadratic energies finding phase equilibria becomes an algebraic problem, and it is possible to calculate some exact solutions.

Let us assume that the non-dimensional energy density functions of both phases are symmetric parabolae ('bilinear material'):

$$f_{\pm}(u') = (u' \pm a)^2. \tag{4.1}$$

In (4.1) the elastic modulus is the same for both components, and a and $-a$ are strains giving the different stress-free stable equilibrium configurations for the two phases. The multi-valued energy (4.1) was originally suggested by Eshelby [10], and has been widely used in the literature.

Equation (3.4) is now linear, and can be solved explicity: the infinite-dimensional part of the problem thus uncouples, and finding extremals reduces to the solution of a system of algebraic equations. This in turn splits into 'a linear subsystem' plus a nonlinear one, reflecting the splitting of the problem into its convex (quadratic, in this case) and non-convex parts noticed earlier. Given c_i, the general solutions of (3.4) in each seperate single-phase interval $[c_i, c_{i+1}]$ are given by linear combinations of suitable expotentials with constant coefficients

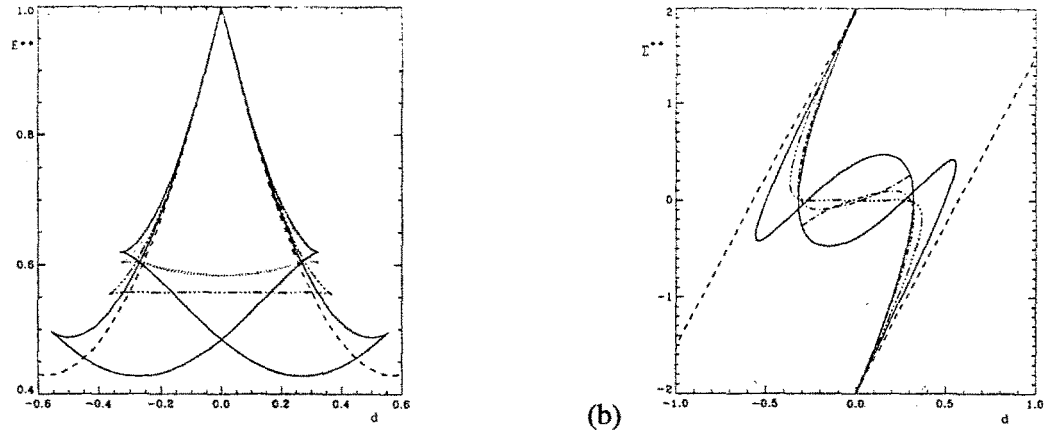

Fig. 3. (a) The calculated N-branches of the effective energy $E_N^{**}(d)$ for the case of symmetric boundary conditions (2.7), for $\alpha = 0.01$ and $\beta = 10$: - - - - - - - $N = 0$; — · · · — $N = 1$; ——— $N = 2$ (sub-branch of centro-symmetric extremals); · · · · · $N = 2$ (sub-branch of non-centro-symmertic extremals). (b) The corresponding branches in the effective stress-strain curves $\Sigma_N^{**}(d)$: - - - - - - - $N = 0$; — · · · — $N = 1$; ——— $N = 2$ (sub-branch of centro-symmetric extremals); — · — · $N = 2$ (sub-branch of non-centro-symmetric extremals).

$a_{h,i}$ with $i = 0, 1, \ldots, N$, and $h = 1, \ldots, 4$, because (3.4) is linear of the fourth order. These solutions must satisfy the boundary conditions (2.5) and (3.7), and are matched at the N transitions points c_i by means of the jump conditions (3.5–3.8). The phase-equilibrium values for the c_i's are then obtained by using the N equations (3.6), which, owing to (4.1), become explicitly

$$u'(c_i) = 0. \tag{4.2}$$

This means that the Maxwell condition (3.6) requires in this case the strain to be *zero* at the transition points c_i (see Figure 2). The jump and boundary conditions (3.5–3.8) give a linear system of $4(N + 1)$ algebraic equations in $4(N + 1)$ unknowns $a_{h,i}$. For any generic choice of the parameters c_i within the appropriate ranges, the solutions

$$a_{h,i} = a_{h,i}(c_1, \ldots, c_N, d, \alpha, \beta), i = 0, 1, \ldots, N, h = 1, \ldots, 4, \tag{4.3}$$

of this linear system are calculated, and the elastic equilibria of the bar are thus completely determined. The coefficients $a_{h,i}$ turn out to depend linearly on d.

The nonlinearity is all concentrated in the problem of finding phase-equilibria, which amounts to solving the N nonlinear algebraic equations (4.2), with unknowns $c_1, \ldots, c_N$. The functions

$$c_i = c_i(d, \alpha, \beta), \quad i = 1, 2, \ldots, N, \tag{4.4}$$

giving the solutions of the N equations (4.2) select, for each d, the phase-equilibrium values for the positions of the transition points. In general, they are non-unique, so that (4.4) is multi-valued.

5. Some Examples

In this section we present some explicit results obtained from the equations in Sections 3 and 4. In all the computations we have set $a = 1$ (see (4.1)) and have used (small) values of α and

β such that the condition $1-4\alpha\beta > 0$ is satisfied. This implies that all four characteristic roots of the Euler–Lagrange equation (3.4) are real and distinct. All the effective energy functions are even due to the symmetry of the energies in (4.1).

5.1. PHASE-EQUILIBRIA WITH NO INTERFACES ($N = 0$)

The phase-equilibria in the 0-branch coincide with the elastic equilibria, and constitute a family of non-homogeneous solutions of the linear equation (3.4) that are always stable. There is a unique solution in u-space, belonging to the 0-branch, for all d (for $d = 0$ it gives the homogeneous solution with identically zero displacements). Nonetheless, the energy $E_0^*(d) \equiv E_0^{**}(d)$ (see (3.1–3.2)) is double-valued; its profile can be seen in Figure 3(a) (dashed line), where only the lowest energy portion of each branch is shown. The corresponding effective stress-strain relation $\Sigma_0^{**}(d)$ is presented in Figure 3(b)(dashed line).

Notice that the minima of $E_0^*(d)$ are always above zero: this happens due to the energy stored in the substratum. In the case of vanishing β (and arbitrary α) we obtain a family of homogeneous deformations whose energy profile reproduces the two original parabolae.

5.2. PHASE-EQUILIBRIA WITH ONE INTERFACE ($N = 1$)

Extremals in the 1-branch have one transition point $c \in [0, 1]$; the multi-valued function (4.3) with $N = 1$, giving the position $c(d)$ of the interface for such phase-equilibria, determines the structure of the 1-branch of extremals, which are non-unique for any generic d within a bounded interval of the d-axis (also determined by the $c - d$ relation).

The 1-branch $E_1^{**}(d)$ of the effective energy is represented in Figure 3(a) by the triangular curve (chain-dot dashed line). For vanishing α and β the lower side of the triangle follows the convex envelope of the original parabolae. The 0- and 1- (and indeed all) branches of extremals, intersect in u-space at the trivial homogeneous solution $u \equiv 0$. Thus all energy branches meet at $d = 0$, as shown in Figure 3(a) for $N = 0, 1, 2$. This is due to the absence of the spinodal region in the energy (4.1). Notice that $u \equiv 0$ is the only common point of intersection of all branches of extremals in u-space, which also implies that all the energy branches meet at $d = 0$, as shown in Figure 4(a) for $N = 0, 1, 2$. This is due to the absence of the spinodal region in the energy (4.1). In fact, the bifurcation diagram similar to the one shown in Figure 3(a) is less singular around the point $d = 0$ in the case of a smooth double-well energy with a spinodal region. For example, for $\beta = 0$, one can show that for the model based on a smooth energy density the branch of the effective energy corresponding to the monotone extremals (the analog of our $E_1^{**}(d)$) has a triangular shape similar to the 1-branch shown in Figure 3(a). However, it bifurcates from the homogeneous branch of the effective energy (the analog of our $E_0^{**}(d)$) and then reconnects with it at two different points (see Figure 4), rather than at one point ($d = 0$), as in the case of the biparabolic energy that we are considering. Also notice that moving away from the solution $u \equiv 0$ (for $d = 0$) along the 1-branch entails the creation and growth of an infinitesimal *nucleus* of new phase from one of the ends of the bar, without overcoming an energy barrier ("second order transition").

Figure 5 presents the effective energy $E_1^*(c, d)$ (see(3.1)) as a function of c for fixed d. One can see that the phase-equilibria giving the lower side of the energy triangle $E_1^{**}(d)$ in Figure 3a (chain dot dashed line) are all *stable*, for they are local minima of $E_1^*(c, d)$. The two upper sides of the triangle are unstable because they correspond to local maxima of $E_1^*(c, d)$

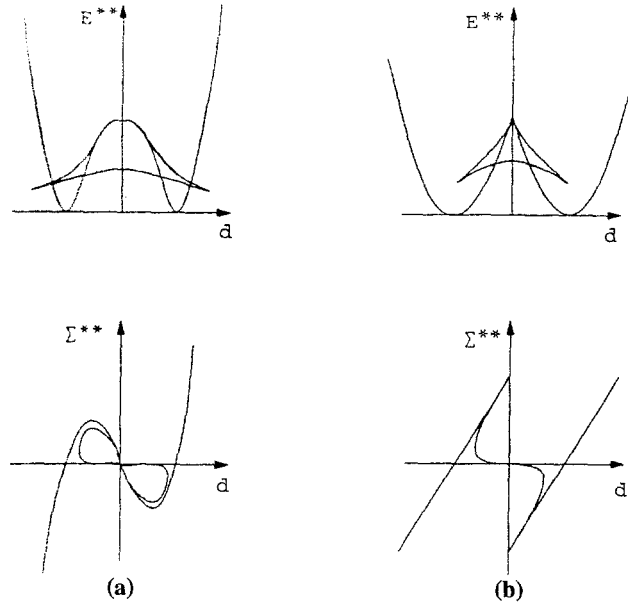

Fig. 4. Schematic diagram showing the effect of the spinodal region on the bifurcation patterns for $\beta = 0$. (a) Effective energies $E_0^{**}(d)$ and $E_1^{**}(d)$ and effective stresses $\Sigma_0^{**}(d)$ and $\Sigma_1^{**}(d)$ for the case of a smooth two-well energy density. (b) The analogous curves corresponding to the branches of homogeneous and monotone equilibria for the bilinear material.

(saddle points in u-space). Notice that even for N as low as 1 there are 'oscillations' in the elastic equilibrium energy of the bar.

5.3. PHASE-EQUILIBRIA WITH TWO INTERFACES ($N = 2$)

Extremals on the 2-branch have two transition points c_1 and c_2 and their bifurcation patterns in u-space are given by the (multi-valued) functions $c_1(d)$ and $c_2(d)$ (see (4.3) for $N = 2$); these also determine the range of existence on the d-axis and the number of phase-equilibria that exist in the 2-branch for each d. The plot of the 2-branch of the equilibrium energy $E_2^{**}(d)$ is shown in Figure 3(a). The multi-valued function $E_2^{**}(d)$ is composed of roughly triangular branches (solid lines) corresponding to centro-symmetric solutions, with bifurcating sub-branches (dotted lines) that correspond to non-centro-symmetric solutions.

At $d = 0$ all sub-branches of $E_2^{**}(d)$ meet at the trivial solution, and they also meet the 0- and 1-branches of the energy, as already noticed. Clearly, the energy branches intersect at points other than $d = 0$; however, this does not mean that the corresponding branches of extremals intersect in u-space, for in fact at these points the different extremals are physically apart and there are *energy barriers* between them (notice the stress drops at those points in the effective stress–strain diagram). The system passing from one equilibrium to the other (for the same $d \neq 0$) reflects the phenomenon of *finite nucleation* at the ends or at the interior of the bar.

Stability can again be assessed from the analysis of the function $E_2^*(c_1, c_2, d)$ for fixed d. It is possible to see that the lowest energy portion of the symmetric sub-branch is stable, i.e. the corresponding solutions are the minima of $E_2^*(c_1, c_2, d)$. All the other extremals, corresponding to the maxima or saddle points of $E_2^*(c_1, c_2, d)$ (all are saddle points in u-space), are unstable phase-equilibria.

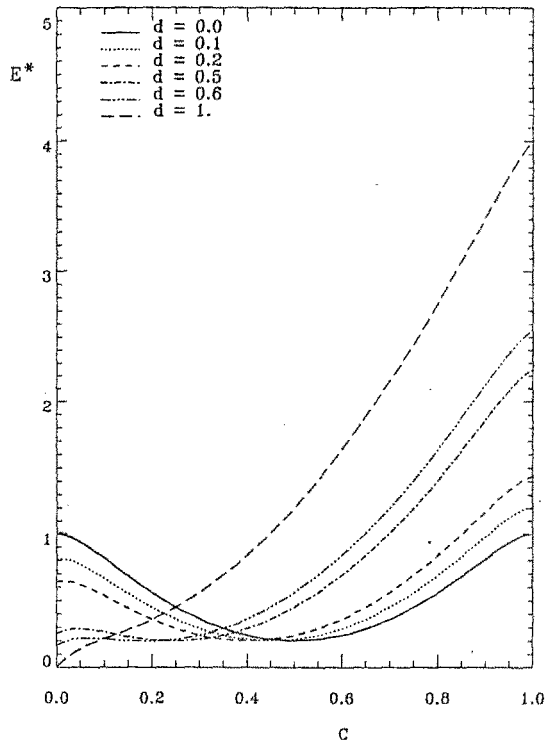

Fig. 5. Profiles of the elastic equilibrium energy $E_1^*(c, d)$ as a function of c, for different values of d ($\alpha = 0.01$ and $\beta = 0.01$). The local minima and maxima give the stable and unstable one-interface phase-equilibria.

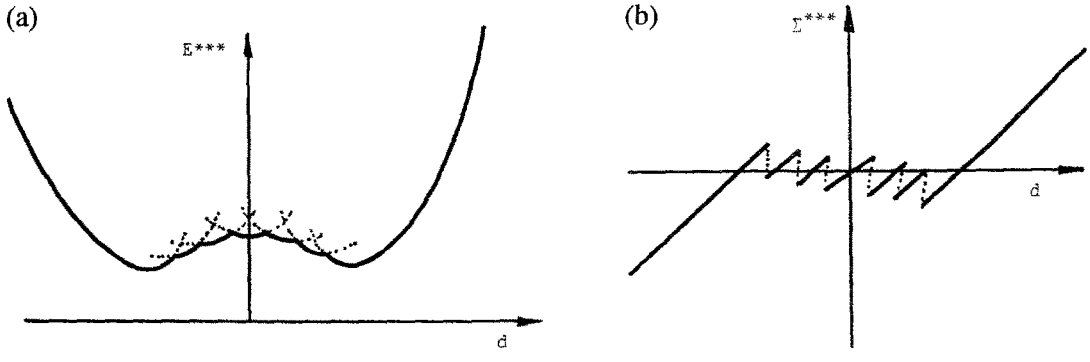

Fig. 6. Maxwell construction for sufficiently small α and β. (a) Absolute-minimum energy $E^{***}(d, \alpha, \beta)$ with non-smooth oscillations. (b) The saw-like discontinuous Maxwell line $\Sigma^{***}(d, \alpha, \beta)$ in the overall stress-strain.

It is interesting to notice that in the various one-dimensional models which extend Ericksen's earlier analysis but neglect surface energy, the energy infimum as a function of total strain is the convex envelope of the original phase energy densities and one observes *infinite* refinement of the microstructures. In our case, however, *finite-scale* microstructures occur as minimizers; moreover, since surface energy is present, the effective energy is higher than in the equivalent system in which surface energy is not considered, and there is a loss of convexity. We can see from our examples that the macroscopic energy is nonetheless at least *locally convex*, at the expense of *reduced smoothness* (see Figure 6(a)). The corresponding

effective stress-strain relation (Maxwell line) is a curve that is only piecewise continuous, with 'jumps' and locally non-negative moduli as in Figure 6(b); see also [9]. This non-smoothness is a result of the branching of the local minimizers, and should be expected in models with a smooth energy (and spinodal region) as well. This is a possible interpretation for the wiggles that are observed in yield and recovery lines in the (quasistatic) uniaxial tension experiments on bars made of multiphase shape-memory alloy (see for instance [6]).

It is also worth noticing how the previous analysis shows that after minimizing out the elastic fields, the energy of an N-branch of equilibria, as a function of the positions of the interfaces, exhibits *multiple* local extrema (different extrema correspond to different phase equilibria in u-space) – see Figure 5. Their number dramatically increases with N. The energy of the bar can thus be viewed as having multiple *macro-oscillations*. On the other hand, in more realistic three-dimensional models more complicated multilayered configurations are considered, which are indeed observed experimentally (see Figure 1(b)). Each next level of microstructure affects the energy by the same mechanism discussed here, and this produces extra *meso-oscillations* of a finer scale in the effective potential, and several internal sub-levels of microstructure might produce several sub-levels of oscillations in the energy. Finally at microlevel (the level of the lattice) the energy as a function of the positions of the interfaces has *micro-oscillations* represented by, say, Pierls barriers. The fact that energy curves with various internal scales of oscillations should be considered (also in relation to some macroscopic aspects of the behaviour of bodies) has only recently been appreciated in the literature. For example, based on the experimental analysis of the 'tip-splitting' mechanism for twin layers, oscillations were added *ad hoc* by Abeyaratne *et al.* [11] to the effective energy, which appears to be among the key elements in their model for the hysteretic behaviour observed in biaxial stretching tests on shape-memory alloys. In general, it is reasonable to relate hysteresis to the possibility that the system gets locked in metastable equilibria; for instance, the potential wells created by meso-oscillations (which this model does not take into account) could make elastic equilibria at least metastable. This effect might be of importance in the interpretation of the recent experimental tests exploring the interior of the hysteresis loop by Fu *et al.* [7] and Ortín [8].

Acknowledgements

We would like to acknowledge the help of A. Polyakov and K. Hane with the numerical computations that led to some of the figures presented in this paper, as well as I. Müller and D. Schryvers for providing the micrographs shown in Figure 1. We appreciate helpful discussion with S. Müller, G. Barenblatt and M. Lanza de Cristoforis, and we thank the Italian CNR for partial financial support. Finally, we would like to thank each of our Institutions for warm hospitality provided to both of us during much of our work.

References

1. Ericksen, J.L. 'Equilibrium of bars', *J. Elasticity*, **5** (1975) 191–202.
2. James, R.D. 'Deformation of shape-memory materials', in *Mat. Res. Soc. Symp. Proc.*, Liu C.Y., Kunsmann, H., Otsuka, K., Wuttig, M. (eds.), **246**, (1992) 81–90.
3. Truskinovsky, L., and Zanzotto, G. 'Ericksen's bar revisited', in preparation.
4. Müller, S. 'Minimizing sequences for nonconvex functionals, phase transitions and singular perturbations', in Kirchgässner, K. (ed.), *Problems Involving Change of Type, Lecture Notes in Physics*, vol. **359**, Springer, Berlin, (1990), pp. 31–44.
5. Müller, S. 'Singular perturbation as a selection criterion for periodic minimizing sequences', *Calculus of variations*, **1** (1993) 169–204.

7. Fu, S., Müller, I., and Xu, H. 'The interior of the pseudoelastic hysteresis', *Mat. Res. Soc. Symp. Proc.* Liu, C.Y., Kunsmann, H., Otsuka, K., Wuttig, M. (eds.) **246**, (1992) 39–42.
8. Ortín, J. 'Preisach modeling of hysteresis for a pseudoelastic Cu-Zn-Al single crystal', *J. Appl. Phys.*, **71** (1992) 1454–1461.
9. Fedelich, B., and Zanzotto, G., 'Hysteresis in discrete systems of possibly interacting elements with a two-well energy', *J. Nonlin. Sci.*, **2** (1992) 319–342.
10. Eshelby, J.D. 'The continuum theory of lattice defects', *Solids State Phys.* **3** (1956) 79–144.
11. Abeyaratne, R., Chu, C., and James, R.D. 'Kinetics and hysteresis in martensitic single crystals', in Brinson, L.C., Moran, B. (eds), *Mechanics of phase transformations and shape-memory alloys*, AMD-Vol. 189, ASME 1994.
12. Schryvers, D., Ma, Y., Toth, L., and Tanner, L. 'Electron microscopy study of the formation of Ni_5Al_3 in a $Ni_{62.5}Al_{37.5}$ B2 alloy. II: plate crystallography', *Acta Metall. Mater.* (1995), in press.
13. Tan, S., and Xu, H. 'Observations on a CuAlNi single crystal', *Cont. Mech. Thermodyn.*, **2** (1990) 241–244.